Molecular Crystals and Liquid Crystals
Publication details, including instructions for authors and subscription information:
http://www.tandfonline.com/loi/gmcl16

Theoretical Investigation of the Shear Flow of Nematic Liquid Crystals with the Leslie Viscosity $\alpha_3 > 0$: Hydrodynamic Analogue of First Order Phase Transitions

T. Carlsson [a]
[a] Institute of Theoretical Physics, Chalmers University of Technology, S-412 96, Goteborg, Sweden
Version of record first published: 20 Apr 2011.

To cite this article: T. Carlsson (1984): Theoretical Investigation of the Shear Flow of Nematic Liquid Crystals with the Leslie Viscosity $\alpha_3 > 0$: Hydrodynamic Analogue of First Order Phase Transitions, Molecular Crystals and Liquid Crystals, 104:3-4, 307-334

To link to this article: http://dx.doi.org/10.1080/00268948408070434

Mol. Cryst. Liq. Cryst., 1984, Vol. 104, pp. 307–334
0026-8941/84/1044–0307/$18.50/0

Printed in the United States of America

Theoretical Investigation of the Shear Flow of Nematic Liquid Crystals with the Leslie Viscosity $\alpha_3 > 0$: Hydrodynamic Analogue of First Order Phase Transitions

T. CARLSSON

Institute of Theoretical Physics, Chalmers University of Technology, S-412 96 Göteborg, Sweden

(Received May 3, 1983; in final form September 6, 1983)

The shear flow of nematic liquid crystals with a positive value of the Leslie viscosity α_3 is studied theoretically. Under the assumption that the director will remain in the plane of shear, the equations governing the flow are solved numerically and the director- and velocity-profile are calculated. The validity of this "in-plane" assumption is discussed, and it is shown that there are at least two situations where it is correct.

For some values of the shear the solution of the equations is multi-valued. By study of the entropy production of the system it is deduced which one of these solutions will be adopted by the system. It is also demonstrated that as a consequence of these multi-valued solutions the system in some cases will behave like a system is undergoing a first-order phase transition.

I. INTRODUCTION

The flow behaviour of nematic liquid crystals can be divided into two different cases depending on the signs of the two Leslie viscosities α_2 and α_3. To give a brief introduction to the subject, let us focus our attention on the behaviour of the liquid crystal in shear flow defining the coordinates as shown in Figure 1. The liquid crystal is confined within two glass plates, distance d apart, both parallel to the xy-plane. The lower one is at rest while the upper one moves with the velocity v_0 in the x-direction. The director is characterized by the polar angles θ

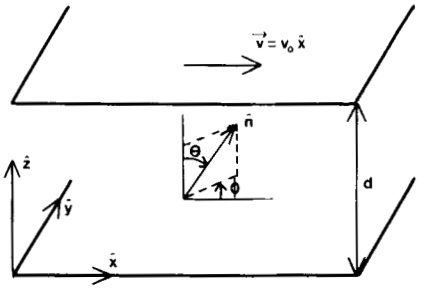

FIGURE 1 Geometry of the general problem. The liquid crystal is confined between two glass plates, both parallel to the xy-plane, distance d apart. The lower one is at rest while the upper one is moved in the x-direction with the velocity v_0. The director is characterized by the polar angles θ and ϕ where θ is the angle between the director and the z-axis and ϕ is the angle between the projection of the director in the xy-plane and the x-axis. The values of θ and ϕ are determined—at every specified set of external conditions—by five viscosity coefficients and three elastic constants.

and ϕ according to the Figure. The two different situations which can occur are now discussed.

Case a: $\alpha_2\alpha_3 > 0$. If α_2 and α_3 are of the same sign the situation is simple and well understood both theoretically and experimentally. Let us consider a homogeneous sample where the boundary conditions give a preferred direction for the director which is assumed to be within the xz-plane ($\phi = 0$). Shearing this sample in the x-direction will cause the director to vary as a function of z still remaining in the plane of shear (i.e. $\theta = \theta(z)$, $\phi = 0$). For high enough shear rates, θ will reach a saturation value (the flow alignment angle) in the bulk of the sample. Near the boundaries we get a transition region where θ varies continuously from the value defined by the boundary conditions to the bulk value. This behaviour is adopted by almost all nematic liquid crystals known at present. In these cases α_2 and α_3 are both negative with $|\alpha_2| > |\alpha_3|$ (the last inequality follows from a thermodynamic condition which must be fulfilled—see Eq. (II.6)). The case when α_2 and α_3 are both positive would also give rise to flow alignment but, up to now, has not been experimentally found. The possibility that nematics consisting of disc like molecules would belong to this class has recently been suggested by the author.[1,2]

Case b: $\alpha_2\alpha_3 < 0$. During the last years some nematic liquid crystals where α_3 is positive and α_2 is negative have been reported in the literature (the case when α_2 is positive and α_3 is negative is prohibited by the inequality (II.6)). Among those is 8CB (octyl-cyano-biphenyl)[3].

In this case flow alignment does not occur and the situation is much more complicated. Some different suggestions for what is happening in this case have been proposed. One suggestion is that a nonstationary state appears,[4] i.e. the time derivative of the director is always nonzero. Another suggestion is that a stationary flow develops, with a value of θ which grows without limit as the shear rate is increased.[5] This behaviour is commonly denoted tumbling. This tumbled state has also been studied by Manneville,[6] whose calculations agree with the calculations presented in this work. We finally mention the work by Pikin,[7] who studied Couette flow of nematic liquid crystals theoretically. A complication of the analysis of this tumbled state is that for high shear rates it lacks stability against fluctuations of the director out of the shearing plane.[8] Taking this into account when analysing the flow we must, for high enough shear rates, not only determine $\theta(z)$ but also $\phi(z)$ in order to describe the flow completely.

The aim of this work is to study the flow behaviour of the nematic liquid crystals when α_3 is positive. We shall be interested in analysing the tumbled state thus assuming that the director remains in the plane of shear. As discussed above this is a simplification of reality. To study the flow behaviour under this restriction should however be a good starting point for understanding these peculiar systems completely. In Section IV we will also show that there are at least two experimental situations where one could expect the director to remain in the plane of shear even for high shear rates. This assures that the calculations are not purely academic. We proceed in the following way. In Section II we develop the general time dependent director equation assuming that the director remains in the plane of shear. We introduce the viscosity function $g(\theta)$ and discuss the various viscosities which are of relevance in the problem. We then use the scaling properties of the equations to reformulate the problem in a way more convenient for numerical solution. We next establish the stationary solutions of the director equation. First we deduce an exact solution in one special case ($K_1 = K_3$ and $\alpha_3 = -\alpha_2$). We then solve the general problem in two steps. The director equation is a nonlinear second order differential equation governing $\theta(z)$. The first integral of this can be obtained analytically determining $d\theta/dz$ as a function of θ. A numerical integration then yields $\theta(z)$. As we shall see, under some circumstances, the flow will develop some instabilities which makes it behave like a system undergoing a first order phase transition. To understand this behaviour we also study the entropy production of the flow. In Section IV at last we discuss the general features of the results. We also describe two experimental situations where the assumption that the director remains in the plane of shear is valid.

II. THE GOVERNING EQUATIONS

In this Section we develop the general equations which governs the flow behaviour of nematic liquid crystals. Assuming the director to remain in the plane of shear the situation is pictured in Figure 2. Our goal is to calculate the variation of the director $\theta(z)$ and the local velocity $v(z)$ when the lower plate is at rest while the upper one is moved. When studying the motion of the upper plate there are two quantities that are of importance. One is its velocity v_0 and the other is the force applied per unit area, τ. These two are of course not independent of each other but will be connected through the viscosity coefficients. Which one of v_0 and τ that shall be regarded as fixed and which one that has to be calculated is a matter of the experimental situation. If we regulate the speed of the upper plate, v_0 is fixed and τ adjusts itself to its proper value. If on the other hand we use a force gauge τ will be fixed while v_0 will be the dependent quantity. Experimentally, the first situation—v_0 fixed—is the more accessible one.

The director equation can be expressed as a balance-of-torque equation and we first study the matter of torques in nematic liquid crystals.

II.1. Torques in nematic liquid crystals

The situation in Figure 2 is obtained as a balance of the elastic and the viscous torque exerted on the director. In this case the elastic torque

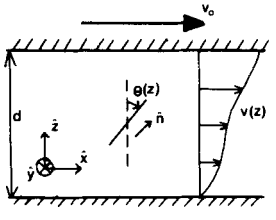

FIGURE 2 Coordinates in the in-plane problem. The lower plate is at rest while the upper one is moved in the x-direction with the velocity v_0. The z-direction is normal to the plates and the y-axis is pointing inwards. The angle which the director makes with the z-axis is denoted θ counting θ positive for a clockwise rotation. The aim of the calculation is to determine $\theta(z)$ and $v(z)$ for a given value for v_0. In the in-plane problem the director is a function of one variable the value of which is determined, except by the five viscosity coefficients, by two instead of all three of the elastic constants.

Γ_y^{el} can be expressed as[9]

$$\Gamma_y^{el} = h(\theta)\frac{d^2\theta}{dz^2} + \frac{1}{2}h'(\theta)\left(\frac{d\theta}{dz}\right)^2 \tag{II.1}$$

where $h(\theta)$ is given by

$$h(\theta) = K_1\sin^2\theta + K_3\cos^2\theta \tag{II.2}$$

K_1 and K_3 are the splay and bend elastic constants.

The viscous torque can be divided into two parts

$$\Gamma_y^v = \Gamma_y^r + \Gamma_y^s \tag{II.3}$$

The rotational part, Γ_y^r, is the torque proportional to the angular velocity of the director, and will not be present in a stationary state. The other part, Γ_y^s, will be called the shearing torque and is due to the shear of the liquid crystal. The viscous torques are given by[9,10]

$$\Gamma_y^s = \left(\alpha_3\sin^2\theta - \alpha_2\cos^2\theta\right)\frac{dv}{dz} \tag{II.4}$$

$$\Gamma_y^r = -\gamma_1\frac{\partial\theta}{\partial t} \tag{II.5}$$

where dv/dz is the local shear.

The viscosity coefficient γ_1 can be shown[11] by thermodynamical arguments to be always positive and is given by

$$\gamma_1 = \alpha_3 - \alpha_2 \geq 0 \tag{II.6}$$

This guarantees that the rotational torque will act as a frictional damping torque against a given rotation of the director.

II.2. The viscous function

In order to get a usable expression for the shearing torque given by Eq. (II.4) we must know the magnitude of the local shear dv/dz. This is connected to the shearing force per unit area τ and the angle θ through a viscous function $g(\theta)$ according to[9]

$$\frac{dv}{dz} = \frac{\tau}{g(\theta)} \tag{II.7}$$

where $g(\theta)$ is given by

$$2g(\theta) = 2\alpha_1\cos^2\theta\sin^2\theta + (\alpha_3 + \alpha_6)\sin^2\theta + (\alpha_5 - \alpha_2)\cos^2\theta + \alpha_4 \tag{II.8}$$

For a full description of the problem we have introduced the six Leslie viscosities α_i ($i = 1$–6). Of these only five are independent due to an Onsager relation first derived by Parodi.[12]

$$\alpha_6 - \alpha_5 = \alpha_2 + \alpha_3 \tag{II.9}$$

In many cases certain combinations of the viscosity coefficients are of interest rather than the coefficients themselves. Two combinations which will turn up to be of interest in this work are the ones commonly denoted by η_1 and η_2.

$$\eta_1 = \tfrac{1}{2}(-\alpha_2 + \alpha_4 + \alpha_5) \geq 0 \tag{II.10}$$

$$\eta_2 = \tfrac{1}{2}(\alpha_3 + \alpha_4 + \alpha_6) \geq 0 \tag{II.11}$$

These expressions are obtained by letting θ be equal to zero (η_1) or 90° (η_2) respectively in Eq. (II.8). Thus η_1 and η_2 are the viscosities measured in a shear flow experiment if the director is constrained to lie perpendicular to the glass plates or in the flow direction as pictured in Figure 3. As the viscous function must be positive definite we can justify[13] the inequalities in Eqs. (II.10) and (II.11).

We now make one approximation commonly made in this kind of problems by neglecting the term $2\alpha_1\cos^2\theta\sin^2\theta$ in the expression for $2g(\theta)$. This approximation was first suggested by MacSithig and Currie.[14] We then rewrite Eq. (II.8) using the Parodi Relation Eq.

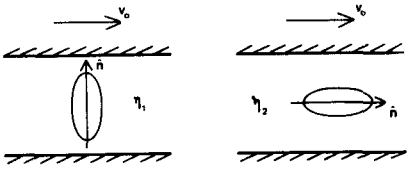

FIGURE 3 The meaning of the viscosities η_1 and η_2. η_1 is the value of the viscous function when θ is put equal to zero ($\eta_1 = g(\theta = 0°)$) while η_2 is the value which one obtains when θ is put equal to 90° ($\eta_2 = g(\theta = 90°)$). η_1 and η_2 are two of the wiesowicz viscosities.

(II.9) as

$$2g(\theta) \simeq \alpha_3 + \alpha_4 + \alpha_6 - 2(\alpha_2 + \alpha_3)\cos^2\theta \tag{II.12}$$

Using Eq. (II.11) we now write

$$g(\theta) \simeq \eta_2 - (\alpha_2 + \alpha_3)\cos^2\theta \tag{II.13}$$

This is the form of the viscous function which will be used below.

II.3. The balance of torque equation

Defining J as the moment of inertia per unit volume of the liquid crystal we can write the equation of motion for the director

$$J\frac{d^2\theta}{dt^2} = \Gamma_y^{el} + \Gamma_y^{v} \tag{II.14}$$

It is easy to show[15] that the moment of inertia term is completely negligible in this case. Looking for stationary solutions we also put $\partial\theta/\partial t$ equal to zero and so end up with the following director equation

$$h(\theta)\frac{d^2\theta}{dz^2} + \frac{1}{2}h'(\theta)\left(\frac{d\theta}{dz}\right)^2 + \left(\alpha_3\sin^2\theta - \alpha_2\cos^2\theta\right)\frac{dv}{dz} = 0 \tag{II.15}$$

By Eqs. (II.7) and (II.13) we can write dv/dz as

$$\frac{dv}{dz} = \frac{\tau}{\eta_2 - (\alpha_2 + \alpha_3)\cos^2\theta} \tag{II.16}$$

Specifying the sample thickness d we now have to solve Eqs. (II.15) and (II.16) simultaneously. We must also regard either v_0 or τ as fixed (depending on which way we perform the experiment as discussed before) while the other will be deduced while solving the equations.

II.4. Scaling analysis

In order to make the numerical solutions of Eqs. (II.15) and (II.16) more general and also easier to perform we use the scaling properties of the equations which was first discussed by Ericksen[16] and introduce

the following scaled quantities

$$\bar{z} = \frac{z}{d} \tag{II.17}$$

$$\bar{v} = vd \tag{II.18}$$

$$\bar{\tau} = \tau d^2 \tag{II.19}$$

Eqs. (II.17) and (II.18) implies

$$\frac{dv}{dz} = \frac{1}{d^2}\frac{d\bar{v}}{d\bar{z}} \tag{II.20}$$

Substituting Eqs. (II.17), (II.18), (II.19) and (II.20) into Eqs. (II.15) and (II.16) give

$$h(\theta)\frac{d^2\theta}{d\bar{z}^2} + \frac{1}{2}h'(\theta)\cdot\left(\frac{d\theta}{d\bar{z}}\right)^2 + \left(\alpha_3\sin^2\theta - \alpha_2\cos^2\theta\right)\frac{d\bar{v}}{d\bar{z}} = 0 \tag{II.21}$$

$$\frac{d\bar{v}}{d\bar{z}} = \frac{\bar{\tau}}{\eta_2 - (\alpha_2 + \alpha_3)\cos^2\theta} \tag{II.22}$$

We have now transformed the problem into the following:
The liquid crystal is confined between two parallel glass plates with unit gap and relative speed $\bar{v}_0$ given by

$$\bar{v}_0 = v_0 d \tag{II.23}$$

On the upper plate the force $\bar{\tau}$ according to Eq. (II.19) is exerted.

If we start the shear with a homeotropic sample and disregard the possibility of forming of disclinations we can conclude by symmetry arguments that $\theta(\bar{z})$ must be an even function around the middle of the sample $\left(\bar{z} = \frac{1}{2}\right)$. The value of θ at this point is denoted by θ_m. If we regard one of the three quantities $\bar{v}_0$, $\bar{\tau}$ and θ_m as known, the other two are determined when solving the Eqs. (II.21) and (II.22). In a real experiment it is $\bar{v}_0$ or $\bar{\tau}$ that can be controlled. As we shall see later however, when solving the equations numerically, we prefer to use θ_m as the input parameter of the problem. We then get the corresponding values of $\bar{v}_0$ and $\bar{\tau}$ as we solve the equations.

II.5. The apparent viscosity

The apparent viscosity η is defined by

$$\eta = \frac{\tau d}{v_0} \tag{II.24}$$

With scaled quantities we get

$$\bar{\eta} = \frac{\bar{\tau}}{\bar{v}_0} \tag{II.25}$$

By Eqs. (II.19) and (II.23) we have

$$\frac{\bar{\tau}}{\bar{v}_0} = \frac{\tau d}{v_0} \tag{II.26}$$

and we conclude that the apparent viscosity in the scaled formulation of the problem is the same as in the real problem, i.e.

$$\bar{\eta} = \eta \tag{II.27}$$

In the general case τ will be a complicated function of v_0 and of the viscosity coefficients α_i. We thus see that the system is non-Newtonian in its behaviour in the sense that η will be a function strongly dependent on the driving force.

III. SOLVING THE EQUATIONS

In this Section we solve Eqs. (II.21) and (II.22) applying the proper boundary conditions. Before solving the equations in the general case, which we have to do numerically, we will solve them in a special case where it can be done analytically. This solution can then be used to check the numerical calculations.

III.1. Solution when $K_1 = K_3$ and $\alpha_3 = -\alpha_2$

The equations will be solvable analytically if the one constant approximation is made and if we study the case $\alpha_3 = -\alpha_2$. The latter assumption is not unrealistic if we consider the normal temperature behaviour of $\alpha_3/|\alpha_2|$ for compounds with α_3 positive: From being negative at high temperatures, $\alpha_3/|\alpha_2|$ goes through zero when decreasing the temperature, finally diverging as the nematic–smectic–A phase–transition temperature is reached.[3] This assures that at some temperature the assumption $\alpha_3 = -\alpha_2$ must be valid.

Introducing further $K = K_1 = K_3$ the Equations (II.21) and (II.22) reduces to

$$K\frac{d^2\theta}{d\bar{z}^2} + \alpha_3\frac{d\bar{v}}{d\bar{z}} = 0 \tag{III.1}$$

$$\frac{d\bar{v}}{d\bar{z}} = \frac{\bar{\tau}}{\eta_2} \tag{III.2}$$

Assuming homeotropic boundary conditions the solution of the equations must fulfill the following conditions

$$\theta(0) = \theta(1) = 0 \tag{III.3}$$

$$\left.\frac{d\theta}{d\bar{z}}\right|_{\bar{z}=\frac{1}{2}} = 0 \tag{III.4}$$

$$\bar{v}(0) = 0 \qquad \bar{v}(1) = \bar{v}_0 \tag{III.5}$$

If the upper plate is moved with the velocity $\bar{v}_0$ then θ_m and $\bar{\tau}$ has to be determined as well as $\theta(\bar{z})$, $\bar{v}(\bar{z})$ and the apparent viscosity $\eta = \bar{\tau}/\bar{v}_0$. Substituting Eq. (III.2) into Eq. (III.1) we get

$$\frac{d^2\theta}{d\bar{z}^2} = -\frac{\bar{\tau}\alpha_3}{K\eta_2} \tag{III.6}$$

Integrating this twice with respect to $\bar{z}$, making use of the conditions (III.3) and (III.4) gives

$$\theta(\bar{z}) = \frac{\bar{\tau}\alpha_3}{2K\eta_2}\bar{z}(1-\bar{z}) \tag{III.7}$$

The maximum tilt, θ_m, appears in the middle of the sample $\left(\theta_m = \theta\left(\frac{1}{2}\right)\right)$ and we get:

$$\theta_m = \frac{\bar{\tau}\alpha_3}{8K\eta_2} \tag{III.8}$$

Substituting Eq. (III.8) into Eq. (III.7) gives

$$\theta = 4\theta_m\bar{z}(1-\bar{z}) \tag{III.9}$$

Finally we must calculate $\bar{\tau}$ as a function of $\bar{v}_0$. Eqs. (III.2) and (III.5) give

$$\int_0^{\bar{v}_0} d\bar{v} = \frac{\bar{\tau}}{\eta_2}\int_0^1 d\bar{z} \tag{III.10}$$

which gives

$$\bar{\tau} = \bar{v}_0\eta_2 \tag{III.11}$$

The velocity profile is now given by integration of Eq. (III.2)

$$\int_0^{\bar{v}} d\bar{v} = \frac{\bar{\tau}}{\eta_2}\int_0^{\bar{z}} d\bar{z} \tag{III.12}$$

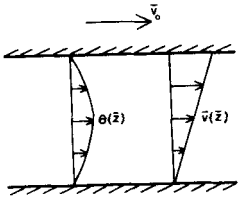

FIGURE 4 Director profile $\theta(\bar{z})$ (Eq. III.9) and velocity profile $\bar{v}(\bar{z})$ (Eq. III.13) in the special case when $K_1 = K_3$ and $\alpha_3 = -\alpha_2$.

Making use of Eq. (III.11) we get

$$\bar{v}(\bar{z}) = \bar{v}_0 \bar{z} \tag{III.13}$$

The apparent viscosity is given by Eqs. (II.25), (II.27) and (III.11) as

$$\eta = \frac{\bar{\tau}}{\bar{v}_0} = \eta_2 \tag{III.14}$$

The solution of the problem is now given by Eqs. (III.8), (III.9), (III.11), (III.13) and (III.14) and is illustrated in Figure 4. In this case the liquid crystal shows a perfect Newtonian behaviour.

III.2. The general solution

In order to solve Eqs. (II.21) and (II.22) in the general case we proceed in two steps. Substituting Eq. (II.22) into Eq. (II.21) gives an equation which we can integrate once. Then we make a numerical integration in order to get $\theta(z)$. Eqs. (II.21) and (II.22) give

$$h(\theta)\frac{d^2\theta}{d\bar{z}^2} + \frac{1}{2}h'(\theta)\left(\frac{d\theta}{d\bar{z}}\right)^2 + \frac{\alpha_3 \sin^2\theta - \alpha_2 \cos^2\theta}{\eta_2 - (\alpha_2 + \alpha_3)\cos^2\theta}\bar{\tau} = 0 \tag{III.15}$$

$$\frac{d\bar{v}}{d\bar{z}} = \frac{\bar{\tau}}{\eta_2 - (\alpha_2 + \alpha_3)\cos^2\theta} \tag{II.22}$$

Assuming homeotropic boundary conditions the solution of the equa-

tions must fulfill the following conditions

$$\theta(0) = \theta(1) = 0 \tag{III.16}$$

$$\theta\left(\tfrac{1}{2}\right) = \theta_m \tag{III.17}$$

$$\left.\frac{d\theta}{d\bar{z}}\right|_{\bar{z}=\frac{1}{2}} = 0 \tag{III.18}$$

$$\bar{v}(0) = 0 \tag{III.19}$$

$$\bar{v}\left(\tfrac{1}{2}\right) = \tfrac{1}{2}\bar{v}_0 \tag{III.20}$$

The conditions (III.18) and (III.20) are due to the symmetry of the solution with respect to the midplane of the sample.

We now solve the equations using θ_m as an input parameter. For each value of θ_m we calculate the corresponding values of $\bar{v}_0$, $\bar{\tau}$ and η as well as the director profile $\theta(\bar{z})$ and the velocity profile $\bar{v}(\bar{z})$. Defining $\bar{u}$ by

$$\bar{u} = \frac{d\theta}{d\bar{z}} \tag{III.21}$$

we can rewrite $d^2\theta/d\bar{z}^2$ as

$$\frac{d^2\theta}{d\bar{z}^2} = \frac{d\bar{u}}{d\bar{z}} = \frac{d\bar{u}}{d\theta}\frac{d\theta}{d\bar{z}} = \bar{u}\frac{d\bar{u}}{d\theta} \tag{III.22}$$

Substituting Eq. (III.22) into Eq. (III.15) we get

$$\frac{1}{2}\frac{d}{d\theta}\left(h(\theta)\bar{u}^2\right) = f(\theta)\bar{\tau} \tag{III.23}$$

where we have defined $f(\theta)$ as

$$f(\theta) = \frac{\alpha_2\cos^2\theta - \alpha_3\sin^2\theta}{\eta_2 - (\alpha_2 + \alpha_3)\cos^2\theta} \tag{III.24}$$

Integrating Eq. (III.23) gives

$$\frac{1}{2\bar{\tau}}h(\theta)\bar{u}^2 = \int f(\theta)\, d\theta + C \tag{III.25}$$

where C is a constant of integration. Performing the integration of $f(\theta)$ using the definitions of η_1 and η_2 in Eqs. (II.10) and (II.11) we get

$$F(\theta) = \int f(\theta)\, d\theta = \left(\frac{\alpha_2}{\sqrt{\eta_1\eta_2}} + \sqrt{\frac{\eta_1}{\eta_2}}\right)\arctan\left(\sqrt{\frac{\eta_2}{\eta_1}}\tan\theta\right) - \theta \tag{III.26}$$

This result has earlier been derived by Currie and MacSithig.[17] Eqs. (III.21), (III.25) and (III.26) now give $d\theta/d\bar{z}$ as

$$\frac{d\theta}{d\bar{z}} = \sqrt{2\bar{\tau}}\,\frac{\sqrt{F(\theta) - F(\theta_m)}}{\sqrt{h(\theta)}} \tag{III.27}$$

where we have determined the constant of integration C by the conditions (III.17) and (III.18) as

$$C = -F(\theta_m) \tag{III.28}$$

Eq. (III.27) is now rewritten as

$$d\bar{z} = \frac{1}{\sqrt{2\bar{\tau}}}\,\frac{d\theta\sqrt{h(\theta)}}{\sqrt{F(\theta) - F(\theta_m)}} \tag{III.29}$$

and together with Eq. (III.16) gives

$$\bar{z}(\theta) = \frac{1}{\sqrt{2\bar{\tau}}}\int_0^{\theta}\frac{\sqrt{h(\theta)}}{\sqrt{F(\theta) - F(\theta_m)}}\,d\theta \tag{III.30}$$

Eq. (III.30) is an implicit expression for $\theta(\bar{z})$.

Before the solution is completed we have to determine $\bar{\tau}$, $\bar{v}_0$ and $\bar{v}(\bar{z})$. Substituting Eq. (III.17) into Eq. (III.30) gives

$$\bar{\tau} = 2\left[\int_0^{\theta_m}\frac{\sqrt{h(\theta)}}{\sqrt{F(\theta) - F(\theta_m)}}\,d\theta\right]^2 \tag{III.31}$$

To determine $\bar{v}(\bar{z})$ and $\bar{v}_0$ we have to use Eq. (II.22) which can be rewritten as

$$d\bar{v} = \frac{\bar{\tau}}{\eta_2 - (\alpha_2 + \alpha_3)\cos^2\theta}\,d\bar{z} \tag{III.32}$$

With $\theta(\bar{z})$ and $\bar{\tau}$ given by Eqs. (III.30) and (III.31) we integrate Eq. (III.32)

$$\bar{v}(\bar{z}) = \int_0^{\bar{z}}\frac{\bar{\tau}}{\eta_2 - (\alpha_2 + \alpha_3)\cos^2\theta(\bar{z})}\,d\bar{z} \tag{III.33}$$

By applying the condition (III.20) on Eq. (III.33) we get $\bar{v}_0$

$$\bar{v}_0 = 2\int_0^{1/2} \frac{\bar{\tau}}{\eta_2 - (\alpha_2 + \alpha_3)\cos^2\theta(\bar{z})} d\bar{z} \qquad \text{(III.34)}$$

The solution of the problem is now given for each value of θ_m by Eqs. (III.30), (III.31), (III.33) and (III.34). The integrals in these equations have to be calculated numerically. We thus need some realistic values for the physical parameters which enter the problem.

III.3. Physical parameters of 8CB

The physical parameters which enter the problem are the four viscosity coefficients α_2, α_3, η_1 and η_2 and the two elastic constants K_1 and K_3. We see in Section II.2 that there are many restrictions which the viscosity coefficients must fulfill. In order to avoid a set of parameters that is unphysical we use an experimentally measured set of viscosity coefficients of 8CB and choose that of Kneppe *et al.*.[18,19] For the elastic constants we use the values measured by Karat and Madhusudana.[20] The values of the physical parameters used in the calculations are summarized in Table I for three different temperatures. In the Table are also given the values of the ratio $\alpha_3/|\alpha_2|$ which is denoted by ξ.

$$\xi = \frac{\alpha_3}{|\alpha_2|} \qquad \text{(III.34)}$$

It turns out that the value of ξ is of utmost importance for the behaviour of the solution of the equations.

III.4. Numerical results

The numerical results are presented in Figures 5 to 13. In Figure 5 is shown the director profile $\theta(\bar{z})$ for five different values of θ_m. In

TABLE I

Values of the physical parameters of 8CB used in this work

		Viscosity coefficients (Kneppe *et al.*[11,12])				Elastic constants (Karat *et al.*[13])	
	$\xi = \alpha_3/\lvert\alpha_2\rvert$	η_1(Pa s)	η_2(Pa s)	α_2(Pa s)	α_3(Pa s)	$K_1 \cdot 10^{11}(N)$	$K_3 \cdot 10^{11}(N)$
$T = 34\,^\circ$C	0.57	0.0967	0.0664	−0.0708	0.0405	1.41	2.09
$T = 35\,^\circ$C	0.20	0.0892	0.0335	−0.0697	0.0140	1.28	1.37
$T = 37\,^\circ$C	0.05	0.0790	0.0233	−0.0588	0.0031	1.03	0.95

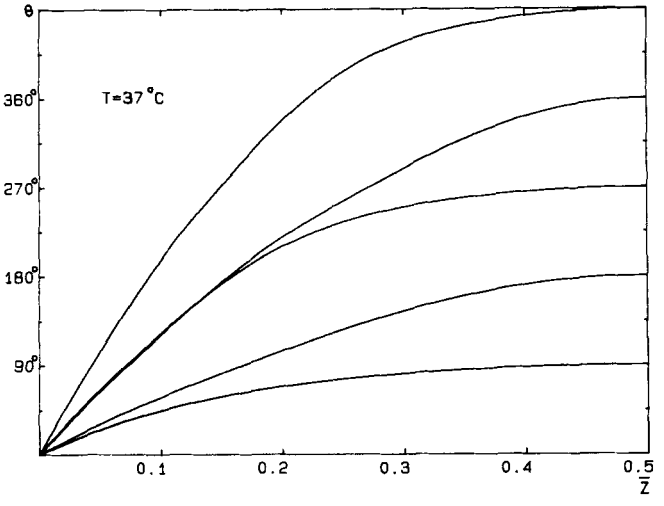

FIGURE 5 θ as function of $\bar{z} = z/d$ calculated for five different values of the maximum tilt angle θ_m. The physical parameters used are those of 8CB at 37 °C which are given in Table I.

Figure 6 we give the corresponding velocity profiles $\bar{v}(\bar{z})$. In both these Figures we have used the physical parameters of 8CB at 37 °C.

In Figure 7 we give θ_m as a function of $\bar{v}_0$ for the three different values of ξ used in the calculations (ξ is defined in Eq. (III.34)). For $\xi = 0.57$, corresponding to the temperature 34 °C the behaviour of θ_m is not very dramatic. In this case θ_m is almost a linear function of $\bar{v}_0$ just as in the exact solution of Section III.1, where ξ was put equal to one. Letting ξ deviate more from one as in the curves of the temperatures 35 °C ($\xi = 0.20$) and 37 °C ($\xi = 0.05$) we see some anomalies in the behaviour of θ_m, which becomes triple- or even multi- for some values of $\bar{v}_0$. This feature of the solution agrees with the calculations presented by Manneville.[6] This multi-valued solution implies that there are many different director- and velocity-profiles which can develop for these values of $\bar{v}_0$. To choose the stable one we have to study the entropy production of the system. This is done in Section III.5. We show that it is always the branch with the smallest value of θ_m which has the least dissipation and thus will be the most stable one. What will happen in an experiment where we increase $\bar{v}_0$ is that the system will undergo discontinuous transitions at the velocities where θ_m makes a jump. This kind of behaviour has been observed experimentally by Cladis and Torza.[4] Figure 8 shows θ_m as a function of $\bar{\tau}$. Again θ_m becomes multi-valued for some values of $\bar{\tau}$ and the system

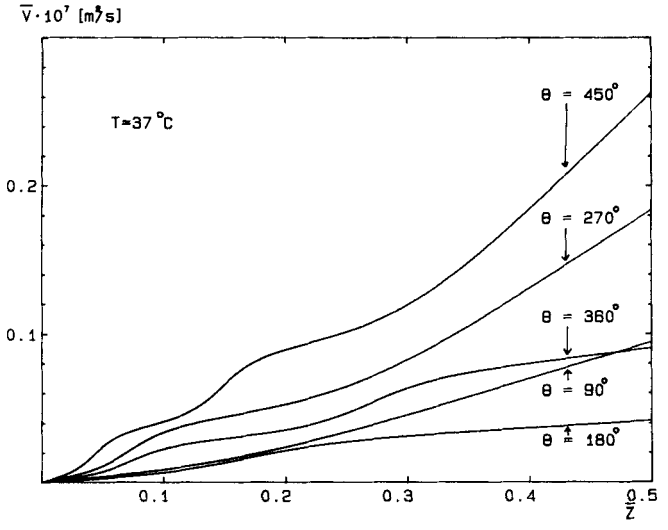

FIGURE 6 $\bar{v} = v/d$ as function of $\bar{z} = z/d$ calculated for the five different values of θ_m that are showed in Fig. 5. The physical parameters used are those of 8CB at 37 °C which are given in Table I.

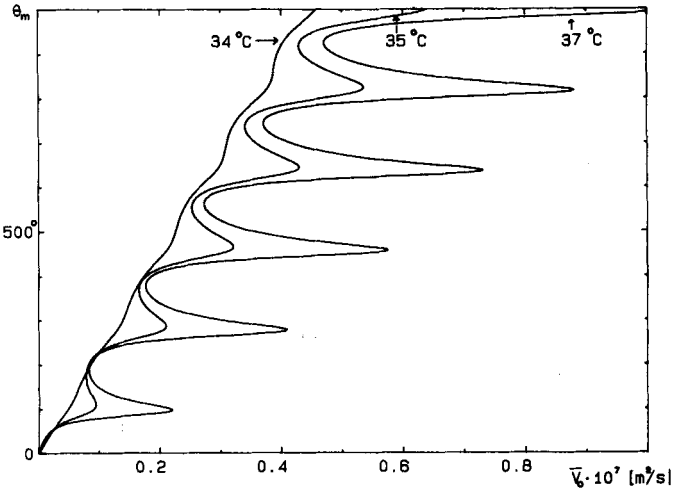

FIGURE 7 θ_m as function of $\bar{v}_0 = v_0/d$ calculated for the three different sets of physical parameters of 8CB which are given in Table I. θ_m is the maximum tilt angle and $\bar{v}_0$ is the scaled velocity of the upper plate.

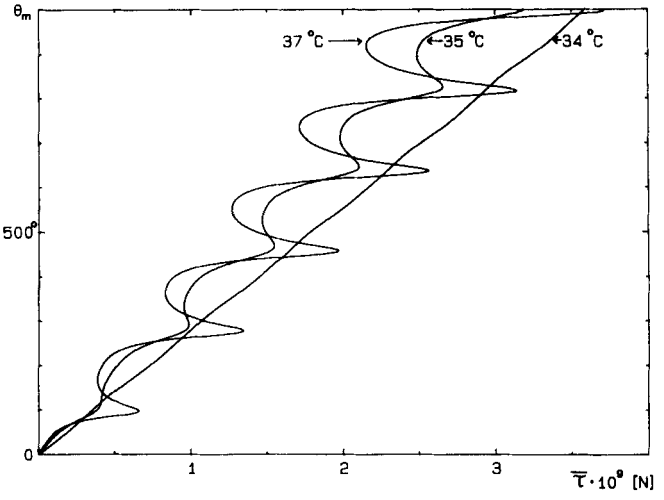

FIGURE 8 θ_m as function of $\bar{\tau} = \tau d^2$ calculated for the three different sets of physical parameters of 8CB which are given in Table I. θ_m is the maximum tilt angle and $\bar{\tau}$ is the scaled force per unit area which is applied on the upper plate.

thus will be forced to undergo discontinuous transitions also in this case. By the study of the entropy production performed in Section III.5 we conclude that in this case it is always the branch with the largest value of θ_m which has the least dissipation and thus will be adopted by the system. The nature of the discontinuities which the system exhibit will be discussed in Section IV.

In Figures 9 and 10 we have plotted η (see Eq. II.25) as a function of $\bar{v}_0$ and $\bar{\tau}$ respectively. We notice the non-Newtonian behaviour; i.e., the apparent viscosity depends strongly on the driving force of the system. We again recognize the discontinuous jumps that the system will undergo at some points. In Figure 9 ($\eta(\bar{v}_0)$) it is always the lowest value of η which will be realized in an experiment. In Figure 10 ($\eta(\bar{\tau})$) however η will always become as large as possible when we have more than one possible value of η for a given value of $\bar{\tau}$. This follows directly from the study of the entropy production of the system performed in Section III.5.

In Figure 11 at last we have plotted $\bar{v}_0$ as a function of $\bar{\tau}$. If one imagine a shear flow experiment performed with a force gauge, measuring the response $\bar{v}_0$ of the upper plate as a function of the applied force $\bar{\tau}$ we see that the system in some cases would act peculiarly. We show in Section III.5 that when we have more than one

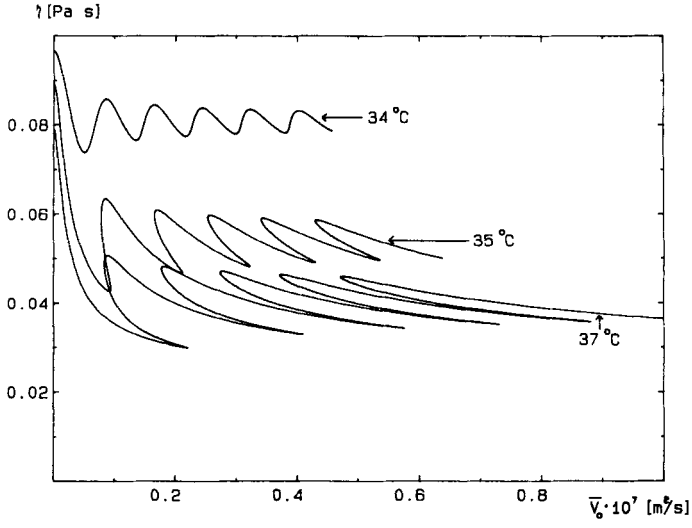

FIGURE 9 The apparent viscosity η as function of $\bar{v}_0 = v_0 d$ calculated for the three different sets of physical parameters of 8CB which are given in Table I. $\bar{v}_0$ is the scaled velocity of the upper plate.

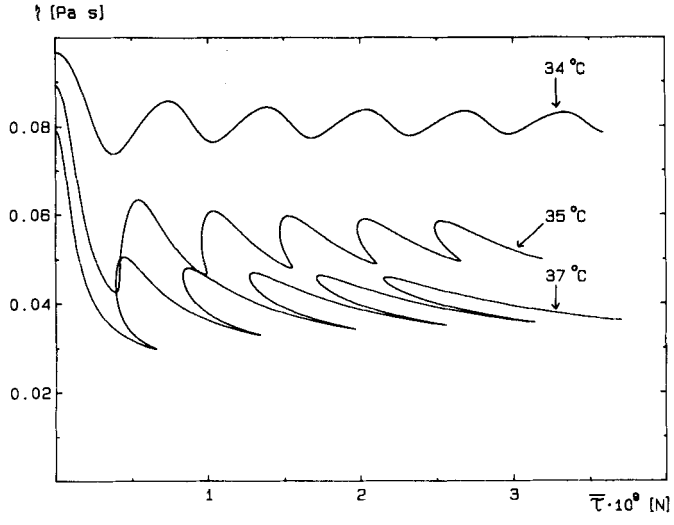

FIGURE 10 The apparent viscosity η as function of $\bar{\tau} = \tau d^2$ calculated for the three different sets of physical parameters of 8CB which are given in Table I. $\bar{\tau}$ is the scaled force per unit area which is applied on the upper plate.

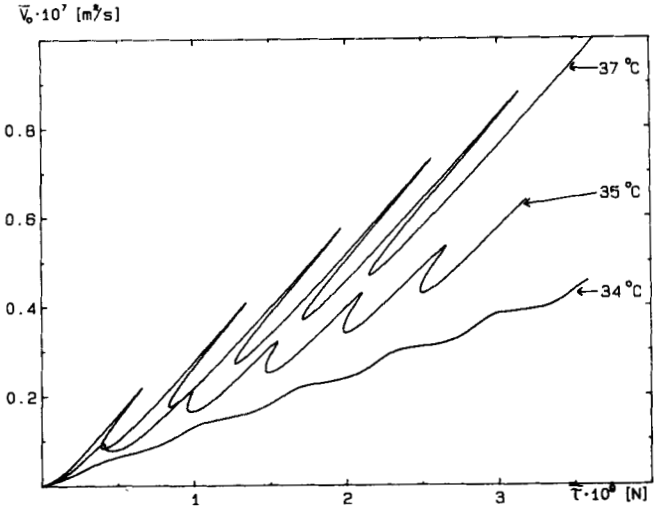

FIGURE 11 $\bar{v}_0 = v_0 d$ as function of $\bar{\tau} = \tau d^2$ calculated for the three different sets of physical parameters of 8CB which are given in Table I. $\bar{v}_0$ is the scaled velocity of the upper plate and $\bar{\tau}$ is the scaled force per unit area which is applied on the upper plate.

possible value of $\bar{v}_0$ for a given value of $\bar{\tau}$ it is always the lowest value of $\bar{v}_0$ which will be realized. This means that we can find regions where increasing the force of the upper plate will cause its velocity to decrease, either continuously or discontinuously. This odd behaviour is of course explained by the fact that when increasing $\bar{\tau}$, the director reorients in such a way that the apparent viscosity increases thus decreasing $\bar{v}_0$ which is connected to η and $\bar{\tau}$ by Eq. (II.25).

III.5. The entropy production

The entropy production per unit volume of the system, σ, is in the absence of temperature gradients given by the expression[11]

$$T\sigma = \alpha_1 (n_i d_{ij} n_j)^2 + 2(\alpha_2 + \alpha_3) n_i d_{ij} N_j + \alpha_4 d_{ij} d_{ij} + (\alpha_5 + \alpha_6) n_i d_{ik} d_{kj} n_j + (\alpha_3 - \alpha_2) N_i N_i \qquad \text{(III.35)}$$

where repeated indices are to be summed over and T is the temperature of the system. n_i are the components of the director and d_{ij} is the strain rate tensor which is given as

$$d_{ij} = \frac{1}{2}\left(\frac{\partial v_i}{\partial x_j} + \frac{\partial v_j}{\partial x_i} \right) \qquad \text{(III.36)}$$

where v_i are the components of the velocity of the fluid. Finally N_i is the rate of change of the director relative the moving fluid

$$\mathbf{N} = \dot{\hat{n}} - \boldsymbol{\omega} \times \hat{n} \tag{III.37}$$

where $\boldsymbol{\omega}$ is the local angular velocity of the fluid given by

$$\boldsymbol{\omega} = \tfrac{1}{2} \nabla \times \hat{n} \tag{III.38}$$

We now apply Eqs. (III.35) to (III.38) assuming the configuration of the flow to be given by Figure 2. The director and velocity fields are then given by

$$n_x = \sin\theta \qquad n_y = 0 \qquad n_z = \cos\theta \tag{III.39}$$

$$v_x = v(z) \qquad v_y = 0 \qquad v_z = 0 \tag{III.40}$$

Studying the stationary state we put all time derivatives equal to zero. The only components of d_{ij} and N_i which are nonzero are given by

$$d_{xz} = d_{zx} = \frac{1}{2}\frac{dv}{dz} \tag{III.41}$$

$$N_x = -\frac{1}{2}\frac{dv}{dz}\cos\theta \tag{III.42}$$

$$N_z = \frac{1}{2}\frac{dv}{dz}\sin\theta \tag{III.43}$$

Substituting Eqs. (III.41) to (III.43) into Eq. (III.35) now gives the required expression for the entropy production per unit volume of the fluid

$$T\sigma = \left(\frac{dv}{dz}\right)^2 g(\theta) \tag{III.44}$$

where $g(\theta)$ is the viscous function already defined in Eq. (II.8). Substituting Eq. (II.7) into Eq. (III.44) we get

$$T\sigma = \tau\frac{dv}{dz} \tag{III.45}$$

and the entropy production per unit area of the fluid is

$$(T\sigma)_{u.a.} = \int_0^d T\sigma\, dz = \tau\int_0^d \frac{dv}{dz}\, dz = \tau v_0 \tag{III.46}$$

By the use of Eq. (II.24) we can rewrite Eq. (III.46) into another very useful expression

$$(T\sigma)_{u.a.} = \frac{\eta v_0^2}{d} = \frac{\tau^2 d}{\eta} \tag{III.47}$$

We are now in the position to decide which flow behaviour that will be adopted by the system in the case where we have more than one solution to the equations for a given value of $\bar{v}_0$ or $\bar{\tau}$. By the principle of minimum entropy production we conclude that it is the solution which minimizes the entropy production which will be adopted by the system. Concerning Figures 9 and 10 where we have plotted the apparent viscosity as a function of $\bar{v}_0$ and $\bar{\tau}$ respectively we draw the following conclusions by the use of Eq. (III.47): If we use $\bar{v}_0$ as the control parameter the entropy production is proportional to η and will thus be minimized by choosing η as small as possible. If on the other hand $\bar{\tau}$ is the control parameter the entropy production is inversely proportional to η and we should choose η as large as possible in order to minimize the entropy production. There might at first sight seem to

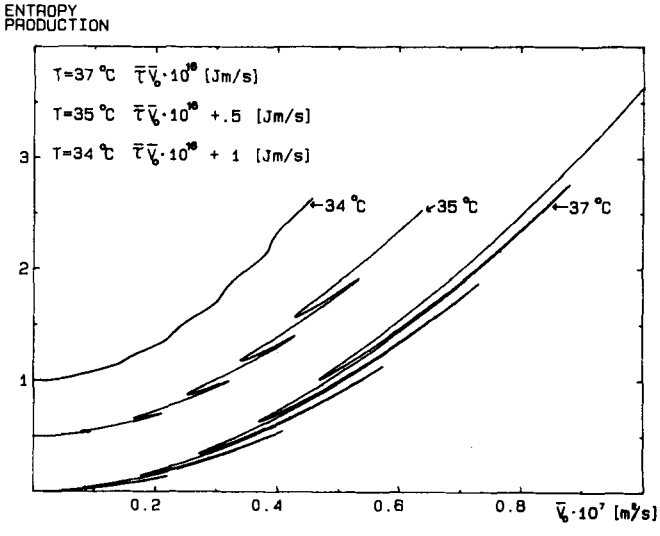

FIGURE 12 The entropy production as function of $\bar{v}_0 = v_0 d$ calculated for the three different sets of physical parameters of 8CB which are given in Table I. $\bar{v}_0$ is the scaled velocity of the upper plate. The graphs are parametrized by θ_m in such a way that be following them from the lower left to the upper right, θ_m increase as we go along them.

be a contradiction in the conclusions drawn above, but it is easy to convince oneself that this is not the case. The entropy production as given by Eq. (III.46) is seen to be simply the product of τ and v_0. If v_0 is fixed and there are more than one value of η corresponding to this value of v_0 we see from Eq. (II.24) that the lowest value of η corresponds to the lowest value of τ and thus to the minimum entropy production. If we on the other hand regard τ as fixed we see again from Eq. (II.24) that choosing η as large as possible will minimize v_0 thus minimizing the entropy production. If we study $\bar{v}(\bar{\tau})$ which is given in Figure 11 or $\bar{\tau}(\bar{v}_0)$ (discussed in Section IV) we can immediately by the use of Eq. (III.46) conclude that it is always the lowest branch of the graphs which will minimize the entropy production. At last we study Figures 7 and 8, where we have given θ_m as a function of $\bar{v}_0$ and τ respectively. To get a better understanding of these figures we first study Figure 12, where we have given the entropy production as a function of $\bar{v}_0$. The graphs in Figure 12 are parametrized by θ_m in such a way that by starting from the bottom left θ_m increase as we go along the graphs. Thus when having more than one possible value of the entropy production for one given value of $\bar{v}_0$ we shall choose the solution with the smallest value of θ_m in order to

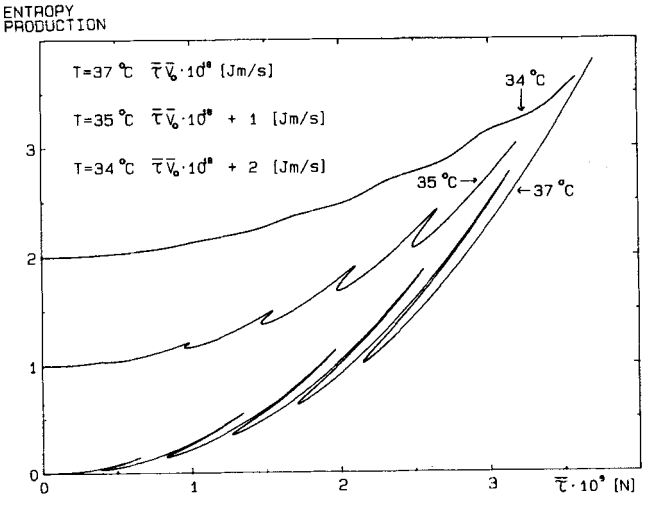

FIGURE 13 The entropy production as function of $\bar{\tau} = \tau d^2$ calculated for the three different sets of physical parameters of 8CB which are given in Table I. $\bar{\tau}$ is the scaled force per unit area which is applied on the upper plate. The graphs are parametrized by θ_m in such a way that by following them from the lower left to the upper right, θ_m increase as we go along them.

minimize the entropy production. We then regard the lower branch to be the most stable one in Figure 7. If we on the other hand study the entropy production as a function of $\bar{\tau}$ (Figure 13) we conclude that in this case the entropy production for a given value of $\bar{\tau}$ will be minimized by choosing θ_m as large as possible, and thus we shall regard the upper branch to be the most stable one in Figure 8.

III.6. Analogue to first order phase transitions

We now imagine an experiment where we control the velocity v_0 of the upper plate. Increasing the velocity from zero, θ_m will increase continuously until we reach a critical velocity which we denote by v_0' (see Figure 14). At this velocity θ_m will make a discontinuous jump. Increasing the velocity further on we will get a new discontinuous jump of θ_m at the velocity v_0'' and so on. If we lower the velocity of the upper plate across one of the critical velocities we can expect the system to follow the upper branch as is indicated in Figure 14. As is shown in Section III.5, this branch represents a state with a larger entropy production than the two lower branches which is obtained for the same value of v_0. We are thus maintaining a metastable "super-

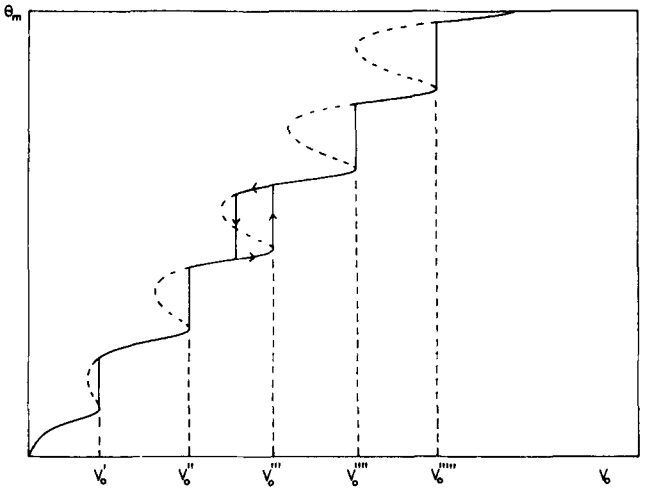

FIGURE 14 Demonstration of the analogue of first order phase transitions. When the velocity of the upper plate v_0 is increased, the maximum tilt angle θ_m (and consequently the director profile $\theta(z)$) will make discontinuous jumps at certain velocities. When decreasing the velocity across one of these critical velocities we can expect the system to maintain a metastable state for some time before it relaxes to the lower branch which is proved to be the solution with the least dissipation.

cooled" state which ultimately must relax to the state with the lowest entropy production. We see that the system behaves just like a system which undergoes a first order phase transition showing effects like supercooling and hysteresis.

IV. DISCUSSION

The study of the flow behaviour of nematic liquid crystals with a positive value of α_3 (α_2 remaining negative) is a problem which has not been discussed very extensively in the literature. A few attempts to analyse the situation theoretically have been made, and also some experiments which report measurements of the viscosity coefficients have been published (see for instance refs. 3, 4, 6, 7, 8, 18, 19), but no real attempts seem to have been made to analyse the flow behaviour completely. In this paper we have tried to gain some understanding of the system by solving the equations governing the flow in the case where the director is assumed to remain in the plane of shear. Of course this is a simplification of reality as discussed before because above a certain value of the shear rate, the flow gets unstable against fluctuations of the director out of the plane of shear. Nevertheless it might be interesting, as a starting point of understanding the system, to study the flow behaviour in this restricted case.

The results of the calculations are presented in Figures 5 to 13 and are discussed in Sections III.4 to III.6. We see that even in this simplified model of the flow, the system exhibits some interesting instabilities connected to the multi-valued solutions of the equations which exist for certain values of v_0 and τ (see Figures 7 and 8). In particular we notice the analogue of first order phase transitions which is discussed in connection to Figure 14.

In Figures 15 and 16 we summarize the results of the calculations in the following way (No units are displayed on the axes, but the figures shall be interpreted as principle ones): If we imagine an experiment where we increase the velocity v_0 of the upper plate Figure 15 shows what would be observed if we measured the maximum tilt angle, the apparent viscosity or the force per unit area exerted on the upper plate. When there are more than one possible solution for the observed quantity as a function of v_0, the stable one has to be chosen corresponding to minimum entropy production as discussed in Section III.5. In Figure 16 we instead show what would be observed if the experiment were performed with a force gauge. One peculiar thing which we notice is that the maximum tilt angles where the instabilities occur are not the same in the two figures but are slightly larger in the

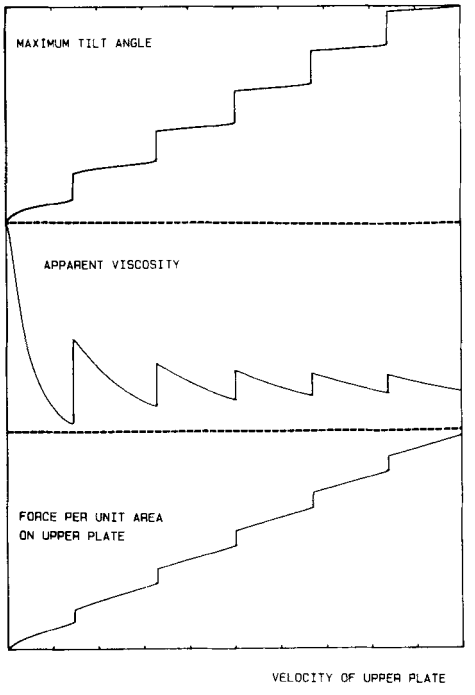

FIGURE 15 Observed values (in a thought experiment) of the maximum tilt angle, the apparent viscosity and the force per unit area exerted on the upper plate as function of the velocity of the upper plate if one perform a shear flow experiment with a velocity gauge (arbitrary units).

case where a velocity gauge is used when performing the experiment. This can be understood in the following way: When performing the experiment with a force gauge we see that when the instability occurs the velocity decreases; first discontinuously and then continuously in a short interval before it begins to increase again (Figure 16, lower part). This means that the system makes a jump into the middle branch of one of the *S*-shaped parts on the $\theta_m(v_0)$ graph. (See left part of Figure 17). As this happens v_0 decreases and θ_m increases. It is then forced to follow this graph to the left (v_0 decreases continuously) until its slope get infinite, and then to the right (v_0 increases). As long as v_0 is smaller than the critical velocity (see Figure 14) we are on a "forbidden" part of the $\theta_m(v_0)$ graph. That it is possible to maintain this situation depends of course on the fact that we now control τ while v_0 have to adjust itself to its proper value corresponding to τ. If instead we perform the experiment with a velocity gauge we will force the system to follow the lower "forbidden" branch on the $\theta_m(\tau)$ graph. When the

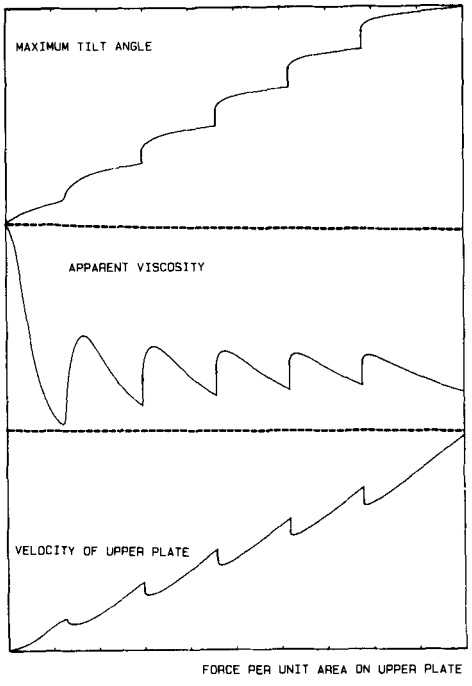

FIGURE 16 Observed values (in a thought experiment) of the maximum tilt angle, the apparent viscosity and the velocity of the upper plate as function of the force per unit area exerted on the upper plate if one perform a shear flow experiment with a force gauge (arbitrary units).

transition sets in τ increases discontinuously taking the system to a point of the upper branch corresponding to a larger value of τ (see right part of Figure 17). By analyzing the calculated data carefully we actually notice that the instability in this case occur exactly when the system is at the point on the $\theta_m(\tau)$ graph where the slope is infinite. We have sketched the way we follow the "forbidden" regions in the $\theta(v_0)$ and $\theta_m(\tau)$ graphs in Figure 17 and indicated by arrows which way the transitions will take the system in the two cases.

In order to make the calculations less pathological we will describe two situations where the assumption that the director remains in the plane of shear is valid. The idea in the first case discussed below is due to discussions with K. Skarp. By synthesizing a compound which exhibits a positive value of α_3 as well as negative dielectric anisotropy we have a possibility of stabilizing the director in the plane of shear. Applying an electric field transverse to the flow would not influence the governing equations but merely introduce a torque tending to

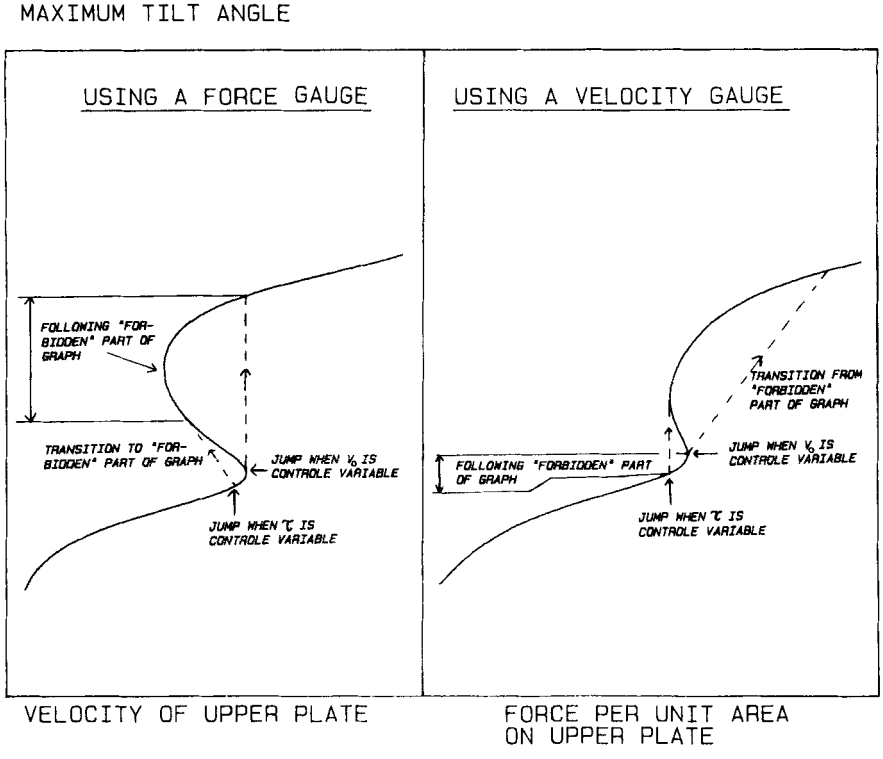

FIGURE 17 Entering and following the "forbidden" part of the $\theta_m(v_0)$ graph when performing a shear flow experiment with a force gauge (left part). Following and leaving the "forbidden" part of the $\theta_m(\tau)$ graph when performing a shear flow experiment with a velocity gauge (right part).

rotate the molecules back into the plane of shear, if a fluctuation brings them out of this. In this way we will suppress the instability which takes the director out of the plane of shear. The other stable case concerns torsional shear flow and the discussion here is due to an argument by Chandrasekhar.[21] In torsional shear flow the liquid crystal is confined between two parallel, circular glass plates; one at rest while the other is rotating. If the instability threshold is reached the director would start to rotate out of the plane of shear. This sudden rotation is coupled to a hydrodynamic flow commonly called back flow.[22] In this case the back flow would be radial, thus creating a pressure drop in the center of the sample. This pressure drop would suppress the back flow and thereby act to stabilize the director against fluctuations out of the plane of shear.

Torsional shear flow experiments have been performed with 8CB by Skarp *et al.*.[3,23] In ref. 23 is described some domain structures which were obtained in one of these experiments. It is the aim of future work to explain these structures by use of the calculations presented here. An investigation of the influence of τ which seems to be the most critical parameter determining the thresholds of the instabilities is under progress. It will also be attempted to get a deeper understanding of the general flow behaviour of nematics with a positive value of α_3 by extending the analysis to the case where the director is not restricted to remain in the plane of shear.

Acknowledgments

The author wishes to express his thanks to K. Skarp for many stimulating discussions of the hydrodynamics of nematic liquid crystals. He also wishes to thank I. Dahl and P. Nordlander for critical reading of the manuscript as well as S. T. Lagerwall for a stimulating and helpful discussion concerning the interpretation of the results calculated.

References

1. T. Carlsson, *Mol. Cryst. Liq. Cryst.*, **89**, 57 (1982).
2. T. Carlsson, *J. Physique*, **44**, 909 (1983).
3. K. Skarp, T. Carlsson, S. T. Lagerwall and B. Stebler, *Mol. Cryst. Liq. Cryst.*, **66**, 199 (1981).
4. P. E. Cladis and S. Torza, *Phys. Rev. Lett.*, **35**, 1283 (1975).
5. P. E. Cladis and S. Torza, Colloid and Interface Science, vol. IV, pages 487–499 (Academic Press 1976).
6. P. Manneville, *Mol. Cryst. Liq. Cryst.*, **70**, 223 (1981).
7. S. A. Pikin, *Sov. Phys.—JETP (Engl. Transl.)*, **38**, 1246 (1974).
8. P. Pieranski, E. Guyon and S. A. Pikin, *J. Physique Colloq.*, **37**, C1, 3 (1976).
9. P. M. Leslie, *Arch. Rat. Mech. Anal.*, **28**, 265 (1968).
10. P. G. de Gennes, The Physics of Liquid Crystals, (Oxford 1975), page 183.
11. F. M. Leslie, *Quart. J. Appl. Math.*, **19**, 357 (1966).
12. O. Parodi, *J. Phys. (Fr.)* **31**, 581 (1970).
13. P. K. Currie, *Arch. Rat. Mech. Anal.*, **37**, 222 (1970).
14. G. P. MacSithig and P. K. Currie, *J. Phys. D*, **10**, 1471 (1977).
15. Orsay Liquid Crystal Group, *J. Chem. Phys.*, **51**, 816 (1969).
16. J. L. Ericksen, *Trans. Soc. Rheol.*, **13**, 9 (1969).
17. P. K. Currie and G. P. MacSithig, *Q. J. Mech. Appl. Math.*, **32**, 499 (1979).
18. H. Kneppe, F. Schneider and N. K. Sharma, *J. Chem. Phys.*, **77**, 3203 (1982).
19. H. Kneppe, F. Schneider and N. K. Sharma, *Ber. Bunsenges. Phys. Chem.*, **85**, 784 (1981).
20. P. P. Karat and N. V. Madhusudana, *Mol. Cryst. Liq. Cryst.*, **40**, 239 (1977).
21. S. Chandrasekhar, (personal communication).
22. S. Chandrasekhar, Liquid Crystals (Cambridge University Press 1977), page 152.
23. K. Skarp, T. Carlsson, I. Dahl, S. T. Lagerwall and B. Stebler, Advances in Liquid Crystal Research and Applications, Ed. L. Bata, (Pergamon Press, Oxford 1980), pages 573–581.